1-17-2021

Structural Behavior of Self-Compacted Reinforced Concrete Beams Strengthed with Hybrid FRP Systems.

Khaled Heiza
Civil Engineering Department., Minuofyia University., Shbeen El-Kom., Egypt

Follow this and additional works at: https://mej.researchcommons.org/home

STRUCTURAL BEHAVIOR OF SELF-COMPACTED REINFORCED CONCRETE BEAMS STRENGTHED WITH HYBRID FRP SYSTEMS

(السلوك الإنشائي للكمرات الخرسانية المسلحة من الخرسانة ذاتية الدمك والمدعمة باستخدام أنظمة البلميرات المسلحة بالألياف المؤلفة)

Khaled M. Heiza
CIVIL ENGINEERING DEPATMENT, MINUOFYIA UNIVERSITY, SHBEEN EL-KOM, EGYPT.

الملخص العربي

تم في هذا البحث دراسة تحسين ممطولية الكمرات الخرسانية المسلحة المصبوبة بإستخدام الخرسانة ذاتية الدمك المحتوية على كلا من غبار السليكا والغبار المتطاير ناتج محطات الطاقة الكهربية. حيث تم تصميم ثمانية أنظمة مختلفة للتدعيم بإستخدام البوليستر المسلح بالألياف الفيبر جلاس وكذلك ألياف الكربون كلا على حده مع إختلاف عدد طبقات التدعيم وكذلك تم استخدام كلا من ألياف الفيبر جلاس والألياف الكربونية مع بعضها البعض لتدعيم البوليستر في بعض النماذج. بالإضافة إلى إستحداث نوع محلي من ألياف البولي بروبلين للتدعيم بإستخدام البولستر أيضا. كذلك تم إستخدام شرائح من الصلب المجلفن سمك ١، ٢مم لتدعيم تلك الكمرات ناحية الشد بإستخدام مادة الايبوكسي كمادة لاحمة لشرائح الصلب المجلفن. وقد عرض البحث بالتفصيل الأسلوب العملي المعملي المستخدم في تدعيم الكمرات الخرسانية ذاتية الدمك. وجرى إختبار هذه الكمرات حتى الكسر وسجلت قيم حمل التشريخ الأولي وكذلك حمل الإنهيار الكلي والترخيم والتشكل وشكل الانهيار وعدد الشروخ واتساعها ونوع ونموذج الانهيار في طبقات التدعيم المستخدمة. وأوضحت النتائج المعملية أن الخرسانة ذاتية التدفق تتمتع بقدر عظيم من قيم الخواص الميكانيكية التي تميزها عن الخرسانة التقليدية في كلا من خواص الضغط والشد والإنحناء الإستاتيكي. أوضحت الدراسة أيضا أنه بغض النظر عن أسلوب وطريقة التدعيم المقترحة فإن قيم الأحمال القصوى والممطولية تتحسن بصورة ملحوظة في جميع العينات موضوع الدراسة. كذلك إمكانية تحسين خواص الممطولية والتشكل وتكون المفاصل اللدنة في الكمرات الخرسانية المسلحة ذاتية التدفق بإستخدام أنظمة FRP والصلب كلا على حدة كما أوضحت الدراسة المعملية سهولة إستخدام وتطبيق وسائل وأساليب التدعيم الإنشائي الحديث بإستخدام البلميرات المسلحة بالألياف. علاوة على ذلك مهدت تلك الدراسة المعملية للعديد من الدراسات المستقبلية لإعادة إستخدام ألياف شكائر البولي بروبلين ناتج مخلفات مصانع وصوامع الغلال في تدعيم العناصر الخرسانية المسلحة. أوضحت الدراسة النظرية التي أجريت بإستخدام الكود المصري لتصميم وتنفيذ المنشآت الخرسانية المسلحة مقارنة بمعادلات الكود الأمريكي والكود الأوروبي فيما يخص حدود الخرسانة ذاتية الدمك وإمكانية إستنباط العديد من المعادلات الرياضية التي تسهل عمل الباحث في هذا المجال. أوضحت الدراسة النظرية المستخدمة في تصميم نظام التدعيم طبقا للكود الأمريكي لتدعيم المنشآت الخرسانية المسلحة بإستخدام الألياف ACI-440-2R-02. تطابق مع مثيلتها المعملية.

ABSTRACT

Self-compacted concrete (SCC) is a recent application of reinforced concrete. Some properties of this type of concrete are recently studied. In this work the ductility of self-compacted reinforced concrete beams was investigated experimentally. Where nine reinforced concrete beam models 10×20×170 cm were cast and tested till failure .The parameters taken into consideration were the methods of strengthening using FRP and steel systems. Where eight different strengthened methods were used including glass fiber reinforced polyester, carbon fiber wrap reinforced polyester and galvanized steel plates. Recorded measurements including cracking loads, ultimate loads, deflection, rotation and modes of failure. The experimental results show that the self-compacted concrete have a good mechanical properties rather than normal strength concrete. The results indicated that the FRP strengthened systems enhancing ductility behavior of self- compacted concrete beams, increasing cracking loads, ultimate loads, cracking distributions and control modes of failure. Comparison between the experimental results and the theoretical ones using ACI 440-2R-02. was performed and discussed.
Key Words: Self- Compacted; Ductility; FRP; Hybrid; Debonding; Peeling; Deflection; Rotation.

I. INTRODUCTION

During the past decade, the issue of deteriorating infrastructure has become a topic of critical importance in many countries. The introduction of fiber-reinforced polymers FRP in Civil Engineering -structures has progressed at a very rapid rate in recent years. These high-performance materials have a unique properties that make them extremely attractive for a wide range of structural applications. The problem of predicting the stiffness, load capacity, and failure modes of RC members strengthened in bending with bonded steel or carbon-reinforced plastic thin plates have been discussed [1]. The study clears that, beams strengthened by steel plates show a ductile response, mainly due to yielding of the strengthening plate. Debonding starts between the point of load application and the plate. Strengthening of reinforced concrete beams with carbon FRP have been investigated [2]. Clamping or wrapping of the ends of the FRP laminate combined with adhesive bonding is effective in anchoring the laminate [Dat and Monica] [2]. Different local failure modes occur in reinforced concrete beams strengthened by FRP plates have been discussed [3]. The local failure modes prevent strengthened beams from reaching their ultimate flexural capacity and ductility. Mazen et al. [3] concluded that shear and normal stress concentrations near the cut off point of the FRP plate and also flexural cracks must be considered in the design of reinforced concrete beams strengthened with epoxy bonded CFRP plates [3].

Concrete cover delamination in RC beams strengthened with FRP sheets have been investigated by [Antonio Nani et al] [4]. Two mechanisms with the concrete cover delamination failure were observed. It was concluded that, the stirrups spacing did not have a remarkable influence in the concrete cover delamination failure [4]. The problem of FRP – concrete delamination was studied [5]. Where a delamination model is developed, which is numerically solved by finite deference method. It was concluded that the behavior of the typical pull-pull setup, adopted for experimental delamination tests, is characterized by a snap-back branch for FRP-concrete bond lengths greater than the minimum anchorage length [5]. Bond behavior between fiber-reinforced polymer laminates and concrete have been examined by Nakaba et al [6]. It was concluded that, the maximum load increases as the stiffness of FRP increases. Maximum load bond stress is not influenced by the type of FRP, but increases as concrete compressive strength increases. [6].

Modeling of debonding behavior in RC beams strengthened with FRP composites have been investigated by Oral et al [7]. The experimental results indicated that increasing the total interface fracture energy in FRP strengthened beams in terms of anchorage reflects on the performance of the beam. The preliminary proposed modeling approach have a good comparability with the experimental results [7]. Strengthening of concrete beams with mechanically fastened FRP strips have been discussed [8]. Lamanna et al concluded that it was possible to strengthened reinforced concrete T beams by attaching FRP strips with mechanical fasteners [8].

The performance of five 1.5m long reinforced concrete beams strengthened with CFRP plates bonded to their soffits is investigated [9]. Where the effects of plate length on the strength of reinforced concrete beams bonded with CFRP plates were discussed. The modes of failure were, concrete ripping-off between the plate and the longitudinal reinforcing bars at the plate end region and flexural failure [9]. NGUYEN et al [10] proposed a new analytical model, which represents the full interaction between the plate, adhesive and concrete. The results obtained using the developed models were in a very close agreement with experimental data [10]. Safan [11] investigated the efficiency of

GFRP composites in strengthening simply supported reinforced concrete beams designed with insufficient shear capacity. The results indicated that significant increase in the shear strength and improvement in the overall structural behavior of beams with insufficient shear capacity could be achieved by proper application of GFRP wrapping [11]. Taljsten [12] and Bilotti [13] proposed some design guidelines for the strengthening of concrete structures using FRP systems. It was concluded that it is important to compile guidelines since without their existents the consultants will fall back to old proven strengthened methods and FRP's will mostly been used in special cases. Checks on the quality of the execution are necessary for phases that involve the preparation of the surfaces, FRP application and FRP impregnation [12] and [13]. Maria lopez [14] design a modeling approach, based on the finite element method to study the behavior of reinforced concrete beams strengthened with CFRP laminates. The results are compared with the previous experimental tests and a good agreement was observed. The numerical models were able to replicate the failure mechanisms, the global load-deflection response, and the strain distribution along the length of the FRP laminate at the tested beam [14]. DAI JIAN GUO [15] developed some suitable test methods, through which the bond behaviors of FRP sheet-concrete interfaces under different loading conditions and different failure modes can be evaluated. The results show that mode 11, Mode 1 and mix-mode fracture tests for FRP sheet-concrete interfaces can be developed using the proposed models. Selim Baraka et al [16] evaluate the performance of concrete structures strengthened with fiber reinforced plastic composites FRP. It was concluded that the experiments that performed were compared with finite element analysis showed good agreement [16].

2. EXPERIMENTAL WORK

2.1. Materials

The components of SCC concrete used in this research are Portland cement , sand, dolomite, water and admixtures (silica fume, fly ash and vescosity enhancing agent VEA).

The production of self compacted concrete should meets the requirements for workability , flowability ,passing ability and strength development.

2.1.1. Cement

Ordinary Portland cement complies the ESS 373/1991 and ASTM - C 150 standards form Suez company is used in casting all SCC specimens. The cement content is remained constant and equal to 400 Kg/m^3 in all mixes.

2.1.2. Aggregates

Both fine and coarse aggregate used for self-compacted concrete SCC, meet the requirements of ESS 1109/2001 and ASTM-C 33. Fine aggregate with a rounded particle shape and smooth texture have been found to require less mixing water in concrete. For this reasons it is preferable in SCC mixes. The optimum grading of fine aggregate for S.C.C. is determined by its effect on water requirement than on physical packing. The sand used was from Abbasa, the physical properties, and sieve analysis are shown in Table (2). Grading of sand are shown in Table (1) and Fig. (1). The coarse aggregate used is dolomite, obtained from Attaka The physical and mechanical properties complies the ESS 1109/2001 and ASTM-C33 standards. The grading of dolomite is shown in Table (3) and Fig. (2).

2.1.3. Admixtures

Two Types of admixtures (mineral and chemical) were used in this study. Silica fume is a by product resulting from the reduction of high - purity quartz with coal in electric furnace in the production of silicon and Ferro-silicon alloys. In this paper the silica fume content was 10% in addition of cement content Table (4) shows both physical and chemical

properties of silica fume used. The fly ash particles are spherical in shape with smooth surface it acts as balls to lubricate mixtures. In this study fly ash with 10% in addition of cement content was used. Table (5) shows both physical and chemical properties of fly ash.

Viscosity enhancing agent VEA. (Viscocrete 5-400) with 2.5% of cement content was used to maintain the slump constant for SCC mixes, Table (6) show properties of VEA. .

2.1.4. Water

The water used in the mix-was drinking water , which is clean, free from impurities, where water cement ratio W/C is kept at 0.33 in all mixes.

2.2 Design Mix and Mixing Regimen

The absolute volume design method is used to design the SCC mixes, the quantities required to produce 1m^3 of self-compacted concrete could be determined as follows :

$$Wc / \gamma_c + W_{agg} / \gamma_{agg} + W_w / \gamma_w = 1000 \ Liter \qquad (1)$$

Where:

Wc   : is the cement weight (kg)

WW   : is the water weight (kg)

γc   : is the specific gravity of cement

γagg : is the specific gravity of fine and coarse Agg.

γw   : is the specific gravity of water

Table (9) shows the self-compacted concrete mix constituents in kg.

2.2.1. Mixing of concrete

The process of concrete mixing by using mechanical mixer includes the following steps :

Weight of the components carefully, adding coarse Agg., adding fine Agg. to the coarse Agg. Let the mixer working for two minutes. Adding water slurry containing the amount of (silica fume, fly ash and viscosity enhancing agent (viscocrete 5-400)) gradually. Let the mixer working for 4 mints. Coating the molds with a layer of mineral oil. Casting the SCC mixture into the steel cubic, cylindrical and prismatic molds without any mechanical vibration. The specimens were covered immediately after casting and

kept for 24 hrs. They were demoulded and cured in water for 28 days in the lab. room temperature until the test age .

2.2.2. Preparation of the self-compacted reinforced concrete beams specimens.

The forms used to cast the reinforced concrete beams with cross section of 10 × 20 cm and a total length of 170 were wooden forms with fair and smooth surfaces.

After mixing and removal of concrete from the mixer bowel concrete was placed in the wooden form containing the steel reinforcement as shown in Fig. (4) without any internal or external vibration.   -

Reinforced concrete beams were removed from the wooden forms after 2 days then reinforced concrete beams were kept at the curing system for 28 days in the lab. room temperature till the date of testing.

2.3. Static Tests

2.3.1. Compression test

The compression test was carried out on cubes of (10 x 10 x 10 cm) using hydraulic testing machine of 2000 KN capacity.

The compression strength was determined by using the relation.

$$Fc = Pc / Ac \qquad (2)$$

Where:

Pc= crushing load (ton)

Ac= cross section area (cm^2)

2.3.2. Indirect tension test

This test was carried out on standard cylinders of dimension 15 cm in diameter and 30 cm in height using hydraulic testing machine of 2000 KN capacity.

The indirect tensile strength was determined by using the following relation:

$$Ft = 2Pc / \Pi DL \qquad (3)$$

Where:

Pc = crushing load (ton)

D = diameter of cylinder (cm)

L = Height of cylinder (cm)

2.3.3. Flexure test

The test was carried out on standard beam specimens of dimensions (10 x 10 x 50 cm) using hydraulic testing machine of 100 KN capacity.

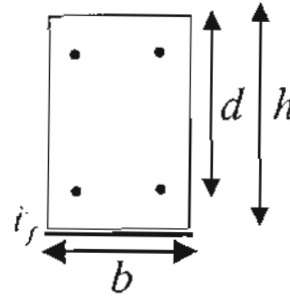$$F_b = MY/I \qquad (4)$$
$$M = PL/4 \qquad (5)$$

Where :

M = bending moment (t.m)

Y = distance from neutral axis (cm)

I = second moment of Inertia (cm^4)

L = span of the beam (cm)

3. DESIGN OF FRP STRENGTHENING SYSTEMS ACCORDING TO ACI 440.2R-02.

Step 1- Calculate the FRP-system design material properties as shown in Tables (7 though 10).

$$f_{fu} = C_f f_{fu}^* \qquad (6)$$
$$\varepsilon_{fu} = C_\varepsilon \varepsilon_{fu}^* \qquad (7)$$

Step 2- Preliminary calculations properties of the concrete as shown in Tables (11 through 13).

β_l from ACI 318-99, Section 10.2.7.3 Ec =57.000-fc

Properties of the existing reinforcing steel.

$$\rho_s{}' = \frac{A_1}{bd} \qquad (8)$$

Properties of the externally bonded FRP reinforcement.

$$A_f = nt_f w_f \qquad (9)$$
$$\rho_f = \frac{A_f}{bd} \qquad (10)$$

Step 3- Determine the existing state of strain on the state of strain on the soffit. The existing state of strain is calculated assuming the beam is cracked and the only loads acting on the beam at the time of the FRP installation are dead loads.

$$\varepsilon_{bi} = \frac{M_m.(h - kd)}{I_{cr} E} \qquad (11)$$

Step 4- Determine the bond-dependent coefficient of the FRP system using Table (10).

$$\kappa_m = \frac{1}{60_{fu}}\left(1 - \frac{nE_f t_f}{175336}\right) \leq 0.90 \qquad (12)$$

Step 5- Estimate C, the depth to the neutral axis. A reasonable initial estimate is 0.20d. The value of the C is adjusted after checking equilibrium.

$$C = 0.20d. \qquad (13)$$

Step 6- Determine the effective level of strain in the FRP reinforcement.

$$\varepsilon_{fe} = 0.003\left(\frac{h - c}{c}\right) - \varepsilon_{bi} \leq k_m \varepsilon_{fu} \qquad (14)$$

Note that for the neutral axis depth selected, concrete crushing would be the failure mode because the first expression in this equation controls. If the second (limiting) expression governed, then FRP failure would be in the failure mode.

Step 7- Calculate the strain in the existing reinforcing steel. The strain in the reinforcing steel can be calculated using similar triangles according to the following equation.

$$\varepsilon_s = (\varepsilon_{fe} + \varepsilon_{bi})\left(\frac{d - c}{h - c}\right) \qquad (15)$$

Step 8- Calculate the stress level in the reinforcing steel and FRP.

$$f_s = E_s \varepsilon_s \le f_y \qquad (16)$$

$$f_{fe} = E_f \varepsilon_{fe} \qquad (17)$$

Step 9- Calculate the internal force resultants and check equilibrium force equilibrium is verified by checking the initial estimate of C, because concrete crushing controls failure, y can be taken as (0.85).

$$c = \frac{A_s f_s + A_f f_{fe}}{\gamma f_c^- \beta_1 b} \qquad (18)$$

Step 10- Calculate design flexural strength of the section, an additional reduction factor. Y f = 0.85, is applied to the contribution of the FRP system.

$$\phi M_n = \phi\left[A_s f_1\left(d - \frac{\beta c}{2}\right) + \Psi A_f f_{fe}\left(h - \frac{\beta c}{2}\right)\right] (19)$$

Step 11- Check service stresses in the reinforcing steel and the FRP. Calculate the elastic depth to the cracked neutral axis by adding the first moment of the areas of the transformed section. This can be simplified for a rectangular beam without compression reinforcement as follows.

$$k = \sqrt{\left(\rho_s \frac{E_s}{E_c} + \rho_f \frac{E_f}{E_c}\right)^2 + 2\left(\rho_s \frac{E_s}{E_c} + \rho_f \frac{E_f}{E_c}\left(\frac{h}{d}\right)\right)} - \left(\rho_s \frac{E_s}{E_c} + \rho_f \frac{E_f}{E_c}\right) (20)$$

Step 12- Calculate the stress level in the reinforcing steel using Eq. (21) and verify that it is less than recommended limit per Eq. (22).

$$f_{s,s} = \frac{\left[M_s + \varepsilon_{bi} A_f \varepsilon_f (h - \frac{kd}{3})\right](d - kd)E_s}{A_s E_s\left(d - \frac{kd}{3}\right)(d - kd) - A_f E_f(h - \frac{kd}{3})(h - kd)} \qquad (21)$$

$$f_{s,s} \le 0.80 f_y \qquad (22)$$

Step 13- Calculate the stress level in the FRP and verify that it is less than creep – rupture stress limit. Assume that the full service load is sustained.

$$f_{f,s} = f_{s,s}\left(\frac{E_f}{E_1}\right)\left(\frac{h - kd}{d - kd}\right) - \varepsilon_{bi} E_f \qquad (23)$$

4. PREPARATION OF THE STRENGTHENING SYSTEMS FOR SELF-COMPACTED REINFORCED CONCRETE BEAMS.

Table (10) and Fig. (3) show the strengthening process sequences used for self-compacted reinforced concrete beams. It is clear that each strengthening system need a special precautions owing to use of different materials like polyester, fiberglass wrapping, carbon fiber wrapping, pp wrapping and finally galvanized steel strips.

Table (7) and (8) show the typical physical, chemical and mechanical properties of constituents of different strengthening systems.

Table (10) show the experimental program of the designed strengthening systems performed on self-compacted reinforced concrete beams.

Fig. (5) illustrate the testing set-up used to perform four point loading flexural test using hydraulic testing machine of 100 KN capacity as shown in Fig. (5). Mechanical dial gauges of 0.01 mm accuracy were used to record the deflections values during the test.

Both initial and final loads were recorded during the test. Finally a new approach was used to record the rotation at right and left hand supports using a special set up as illustrated in Fig. (5). Testing process continued till complete failure and

deflection, rotation, initial load, final load, crack pattern and mode of failure in each strengthening system was recorded.

5. RESULTS AND DISCUSSIONS.
5.1. Static Tests.

Table (11) show the results of the cubic compressive strength f_{cu} for SCC specimens after 28 days. The values of f_{cu} ranged from 333 kg/cm^2 up to 359 kg/cm^2. most of cubes were failed under compressive loads causing shear failure.

Table (12) illustrate the values of indirect tensile strength f_t of SCC specimens.

The values of f_t was ranged from 40 kg/cm^2 up to 47 kg/cm^2. All specimens have a tension failure during testing process, the internal surfaces of the cursing cylinders were very rough.

Table (13) clarifying the results of the flexural strength f_b for SCC test specimens. It clear that f_b ranged from 78.75 kg/cm^2 up to 86.25 kg/cm^2.

5.2. Results of Self-Compacted Reinforced Concrete Beams.
5.2.1. Load-deflection relationship

Table (14), (15) and Fig. (6) shows the summary of the relationships between the loads and deflections for all tested beams, showing the effect of each strengthening method on the deflection behavior of self-compacted reinforced concrete beams.

For control beam (BC) the cracking load was observed at 2 ton form the load level. For other beams the initial cracking loads was ranged from 2.25 ton to 4 ton. Both 1mm and 2mm galvanized steel with 5cm width give the maximum values of cracking loads as shown in Fig. (6) and (8).

For control beam (BC) the initial cracking load equal 2.0 ton and ultimate load equal 5.66 ton. Where for the beam (B1) the initial crack load equal 2.2 ton and ultimate load equal 6.45 ton. The initial cracking load increased by (10%), the ultimate load increased by (14%) and the deflection (Δ) decreased by (2%) compared to the control beam (BC).

For beam (B2) the initial cracking load equal 2.3 ton and ultimate load equal 7.07 ton it was observed that the initial cracking load increased by (15%), the ultimate load increased by (25%) and the deflection (Δ) increased by (20%) compared to the control beam (BC).

For beam (B3) the initial cracking load equal 2.2 ton and ultimate load equal 6.6 ton while the initial cracking load increased by (10%), the ultimate load increased by (16.6%) and the deflection (Δ) increased by (29%) compared to the control beam (BC).

For beam (B4) the initial cracking load equal 2.39 ton and ultimate load equal 6.81 ton where the initial cracking load increased by (19.5%), the ultimate load increased by (20.3%) and the deflection (Δ) decreased by (7%) compared to the control beam (BC).

For beam (B5) the initial cracking load equal 2.1 ton and ultimate load equal 6.14 ton it was cleared that the initial cracking load increased by (5%), the ultimate load increased by (8.5%) and the deflection (Δ) increased by (32%) compared to the control beam (BC).

For beam (B6) the initial cracking load equal 2.5 ton and ultimate load equal 7.75 ton it was observed the initial cracking load increased by (25%), the ultimate load increased by (36.9%) and the deflection(Δ) decreased by (3%) compared to the control beam (BC).

For beam (B7) the initial cracking load equal 3.3 ton and ultimate load equal 8.24 ton while the initial cracking load increased by (65%), the ultimate load increased by (45.6%) and the deflection (Δ) decreased by (5%) compared to the control beam (BC).

For beam (B8) The initial cracking load equal 4 ton and ultimate load equal 7.73 ton it was noticed the initial cracking load increased by (100%), the ultimate load increased by (36.6%) and the deflection(Δ)

decreased by (39%) compared to the control beam (BC).

5.2.2. Load-rotation relationship

Table (14), (15) and Fig. (7) summarize the results of the load rotation relationship for all tested beams showing the effect of each strengthening system on the ductile behavior of self-compacted reinforced concrete beams.

For control beam (BC) the initial cracking load equal 2.0 ton and ultimate load equal 5.66 ton.

For beam (B1) the initial cracking load equal 2.2 ton and ultimate load equal 6.45 ton while the initial cracking load increased by (10%), the ultimate load increased by (14%) and angle of rotation(θ) decreased by (32%) compared to the control beam (BC).

For beam (B2) the initial cracking load equal 2.3 ton and ultimate load equal 7.07 ton it was noticed that the initial cracking load increased by (15%), the ultimate load increased by (25%) and angle of rotation (θ) decreased by (22%) compared to the control beam (BC).

For beam (B3) the initial cracking load equal 2.2 ton and ultimate load equal 6.6 ton where the initial cracking load increased by (10%), the ultimate load increased by (16.6%) and angle of rotation(θ) decreased by(25%) compared to the control beam (BC).

For beam (B4) the initial cracking load equal 2.39 ton and ultimate load equal 6.81 ton while the initial cracking load increased by (19.5%), the ultimate load increased by (20.3%) and angle of rotation(θ) decreased by (25%) compared to the control beam (BC).

For beam (B5) the initial cracking load equal 2.1 ton and ultimate load equal 6.14 ton it was observed that the initial cracking load increased by (5%), the ultimate load increased by (8.5%) and angle of rotation(θ) increased by (22%) compared to the control beam (BC).

For beam (B6) the initial cracking load equal 2.5 ton and ultimate load equal 7.75 ton it was concluded that the initial cracking load increased by (25%), the ultimate load increased by (36.9%) and angle of rotation (θ) decreased by(7%) compared to the control beam (BC).

For beam (B7) the initial cracking load equal 3.3 ton and ultimate load equal 8.24 ton where the initial cracking load increased by (65%), the ultimate load increased by (45.6%) and angle of rotation(θ) decreased by(10%) compared to the control beam (BC).

For beam (B8) The initial cracking load equal 4 ton and ultimate load equal 7.73 ton it was noticed that the initial cracking load increased by (100%), the ultimate load increased by (36.6%) and angle of rotation(θ) decreased by(55%) compared to the control beam (BC).

5.2.3. Initial loads

Table (14), (15) and Fig. (8) shows the values of initial cracking load recorded for each beam owing to the presence of strengthening method. In was noticed that there is an increase in the initial cracking loads for all beams compared to the control beam (BC). The values of initial loads increases were ranged from 5% up to 100% as shown in Table (14), (15) and Fig. (8). The beam (B7) strengthened with 1mm thickness and 50 mm width galvanized steel plate have an increase of 65% of its cracking load compared to the control beam (BC). Beam (B8) have an increase in its cracking loads values by about 100% comparing to the control beam (BC).

5.2.4. Ultimate loads

Table (14), (15) and Fig. (9) illustrates the summary of ultimate load and strengthening systems used in each reinforced self-compacted concrete beams. It is clear that the values of ultimate loads increases for all beams by values ranged from 8.5% up to 45% of its original values recorded from the control beam (BC). Beam (B5) strengthened by four layers of

polypropylene mat fiber with polyester resin recorded an increase in ultimate load by 8.5% from its original value, this can give a chance for PP fiber mat in the future application of reinforced concrete structures strengthening.

5.2.5. Deflection behavior

Table (14), (15) and Fig. (10) show the effect of each strengthening system on the deflection behavior used in each RC beam. For beams (B1, B6, B7, B8) there is some decrease in deflection values ranged from (2% up to 39%) this can attributed to, as the stiffness of the plate increase the deflection decrease i.e. the ductile behavior enhanced. For beams (B2, B3, B4, B5) the values of deflection recorded increases and it's values ranged from (7% up to 32%) this can be attributed to the strengthened methods used in these beams are subjected to some local failure including debonding, peeling and also fiber misalignment during strengthening process so the value of deflection may increase. On the other hand as the stiffness of the FRP layers used is not sufficient owing to high values of concrete strength, the deflection may increase.

5.2.6. Rotation behavior

Table (14), (15) and Fig. (11) illustrate the effect of strengthening system on the rotation behavior of the SC reinforced concrete beams. Its clear that all values of rotation were decreased except for beam (B5) strengthened with 4 layers of PP fiber mat. It was concluded that as the stiffness of strengthening system increase the rotation decrease. i.e. enhancement of the rotation and ductile behavior of the self-compacted reinforced concrete beams. The values of rotation decrease were ranged from 7% up to 55% of its' original values recorded for control beam (BC).

5.2.7. ductility

By using the two equation proposed by the ACI code [19]. The ductility indexes for self-compacted reinforced concrete beams can be calculated as follows.

$$\mu d = \frac{\Delta U}{\Delta Y} \qquad (24)$$

where: μd : is the deflection ductility index

ΔY : deflection at yield stage (mm)

ΔU:ultimate deflection at failure stage (mm)

$$\mu\theta = \frac{\theta U}{\theta Y} \qquad (25)$$

where: $\mu\theta$: is the rotation ductility index

θY: is the yield Rotation (degree)

θU:is the ultimate rotation at failure (degree)

Improvements of the flexural behavior and ductility enhancement were discussed for self-compacted reinforced concrete beams from deflection, rotation and mode of failure point of view. Table (16) illustrates the summery of both deflection and curvature ductility indexes for strengthening reinforced self-compacted concrete beams. It is clear that the values of displacement ductility index μd for control beam (BC) was 5.6, where increased for beams (B1, B3, B4, B5, B6, B8) and decreased for beams (B6 and B7). This can be attributed to some local failure like debonding, peeling, fiber misalignment during testing process. For control beam (BC) the value of rotation ductility $\mu\theta$ was 3.74 where increased for beams (B2, B5, B6 and B7) and decreased for beams (B1, B3, B4 and B8). It was noticed that the max. values of both μd and $\mu\theta$ were observed at beams (B5) that strengthened by 4 layers of PP fiber mat. as shown in Table (16).

5.2.8. Comparison between experimental and theoretical results using ACI-440.2R-02.

Fig. (12) show the comparison between the experimental values of moment acting on the reinforced SCC beams and the theoretical ones proposed by the equations of the ACI-440. 2R-02. Fig. (12) clear that the equations of ACI-440. 2R-02 for design the FRP systems for strengthening RC beams is conservative.

The theoretical values of the moment were ranged from 0.97 t.m up to 1.03 t.m. where for recorded experimental values it ranged from 1.6 t.m up to 2.05 t.m. The max values of differences between both experimental and theoretical values where observed at beam (B7) strengthened by 1mm thickness and 50mm width of the galvanized steel plate. Although the beam (B8) have more stiffness in strengthening system than (B7) but the values of moments in (B7) was larger than in (B8). This can be attributed to some debonding and local failure of the beam (B8) during testing process also peeling effect was observed in beam (B8).

6. MODES OF FAILURE

The process of testing the reinforced self-competed concrete beams included cracking loads, ultimate loads, deflection values, rotation values, crack numbers, crack length, crack propagation, density of cracks and modes of failure were observed in each beam model. It was noticed that for control beam (BC) mode of failure was flexural mode having tension cracks at the mid span of the beam. Where for beams (B1, B2 and B3) strengthened with FRP systems the failure mode was debonding associated with FRP cutting near the maximum loads. For beams (B4 and B6) the failure mode was tension failure associated with some local failure and crushing of concrete in the compression zone. For beam (B5) the failure mode was debonding mode associated with peeling near the supports.

For beams (B7 and B8) the modes of failure was debonding mode with some delaminating between the steel plate, matrix interface and concrete surface. Beam (B8) have some local failure during testing process.

7. CONCLUSIONS.

Form both experimental and theoretical results present in this study it was concluded that:

- All strengthening systems used within this study enhancing the ductile behavior of self-compacted reinforced concrete beams in spite of the details of the strengthening method.
- The stiffness of the strengthening method is the governing factor affecting the behavior of the reinforced self-compacted concrete strengthening beam.
- Polypropylene fiber mat have a good a chance to be future material of RC strengthening.
- Steel plates still have the major wide spared method in strengthening the RC structures.
- Hybrid systems (CFRP + CFRP) considered a good, easy and fast method for rehabilitation retrofitting, repair and strengthening of self-compacted reinforced concrete beams.
- Self-compacted reinforced concrete beams have a better performance than normal and conventional concrete.
- Modes of failure observed in the present work included plate debonding delamination, fiber misalignment, fiber breaking peeling and fiber rupture.

8. REFERENCES

[1] **Alessandra Aprile, et al.,** "Role of Bond in RC Beams Strengthened with Steel and FRP Plates" Journal of Structural Engineering / December 2000.

[2] **Dat, D., Monica, S.,** "Strengthening of Reinforced Concrete Beams with Carbon FRP" Composites in Constructions, Figuefras et al., (2ds), 2001 Swets of Zeitlinger, Lisse, ISBN 90 2651 8587.

[3] **Mazen Almakt, et al.,** "Strengthening of RC Elements by CFRP Plates Local Failure" 2nd International Symposium in Civil Engineering Budapest. 1998.

[4] **Antomio Nani et al.,** "Concrete Cover Delamination in RC Beams Strengthened with FRP Sheets" SP-188, American Concrete Institute, Proc., 4th International Symposium of FRP for Reinforcement of Concrete Structures (FRPRCS4), Baltimore, MD, Nor. PP. 725-735. 1999.

[5] Smazzotti, C., et al., "Delamination of FRP Plate/Sheets Used for Strengthening of r/c Elements" in Bicanic N. et al. (eds), Comp. Modeling of Concrete Structures EURO-C, st. J. in Pongau (Austria) 2004.

[6] Kasumassa, Nakaba, et al., "Bond Behavior Between Fiber-Reinforced Polymer Laminates and Concrete" ACI Structural Journal, V 98, No. 3, May-June 2001.

[7] Oral Buyukoztuzk, et al., "Characterization and Modeling of Debonding in RC Beams Strengthened with FRP Composites" 15th ASCE Engineering Mechanics Conference June 2-5, 2002, Columbia University, New York, NY.

[8] Anthony, Lamanna, et al., "Strengthening of Concrete Beams with Mechanically Fastened FRP Strips" University of Wisconsin Press 2003.

[9] Nguyen, Daiminh, et al., "Effects of Plate Length on the Strength of Reinforced Concrete Beams Bonded with CFRP Plates" EASEC-7 Conference, Kochi, Japan. 1999.

[10] Nguyen, Daiminh, "Interaction Behavior Between Plate-Adhesive – Concrete and Premature Failures of FRP Strengthened Beams" EASEC-7 Conference, Kochi, Japan. 1999.

[11] Mohamed, S., "Shear Strengthening of Reinforced Concrete Beams Using CFRP WRAPS" JL. Egyptian Society of Engineers Vol. 42, No. 4-2003.

[12] Taljsten Bjorn., "FRP Strengthening of Concrete Structures – Design Guidelines in Sweden" 15th ASCE Engineering Mechanics Conference Columbia University, New York, NY. June 2-5, 2002.

[13] Giancarlo, B. and Antonio, P., "Strengthening of Concrete Beams Using Externally Bonded FRP Reinforcement: Numerical Analysis and Design Guidelines" MESC-3 Structural Composites for Infrastructure Applications December 17-20, Aswan, Egypt. 2002.

[14] Maria M. Lopez., "Development of Finite Element Model of RC Beams Strengthened with CFRP Laminates" HBRC Symposium in Composites Cairo Egypt 2003.

[15] DAI, Jan, Guo., "Interfacial Models of Fiber Reinforced Polymer (FRP) Sheets Externally Bonded to Concrete" 15th ASCE Engineering Mechanics Conference, June 2-5, 2002, Columbia University, New York, NY.

[16] Selim Baraka, et al., "Evaluation of the Performance of Concrete Structures Strengthened with FRP Composites" 15th ASCE Engineering Mechanics Conference, June 2-5, Columbia University, New York, NY. 2002.

[17] ACI Committee 318., "Building Code Requirements for Structural Concrete (ACI 318-02) and Commentary (318R-02), "American Concrete Institute, Farmington Hills, Mich., 2002, 369pp.

[18] Euro code 2., Design of Concrete Structures- part 1: General Rules and Rules for Buildings (EC-2). European Prestanderd ENV 1992-1-1:1991, Comte European de Normalization, Brussels, 253pp.

[19] ECCS-203-2001., The Egyptian Code for Design and Construction of Concrete Structures, Housing and Building Research Center, Giza, Egypt 2004.

[20] ACI 440.2 R-02., "Guide for the Design and Construction of Externally Bonded FRP Systems for Strengthening Concrete Structures" American Concrete Institute, October 2002.

Table (1) Grading of Fine Aggregate (Sand).

Sieve size (mm)	Weight retained	Total weight retained	%Retained (by weight)	% of Total Retained (by weight)	% Passing
5.0	0.0	0.00	0.0	0.0	100
2.5	96	96.6	4.83	4.83	95
1.25	210	306.6	10.5	15.33	85
0.62	750	1056.6	37.5	52.83	47
0.31	643.4	1700	32.17	85	15
0.16	300	2000	15.0	100	0.0

Table (2) Physical and Mechanical Properties of Fine Aggregates (Sand).

Property	Measured value
Specific gravity	2.5
Volume weight(t/m^3)	1.792
Fineness modulus	2.6
Voids ratio (%)	33.81 %

Table (3) Grading of Coarse Aggregates (Dolomite).

Sieve size (mm)	Weight retained	Total weight retained	%Retained (by weight)	% Total Retained (by weight)	% Passing
25.4	0.0	0.0	0.0	0.0	100
19.1	750	750	25	25	75
12.7	1200	1950	40	65	35
9.51	360	2310	12	77	23
4.67	540	2850	18	95	5
2.38	150	3000	5.0	100	0

Table (4) Physical and Chemical Properties of Silica Fume.

Physical properties	Value
Color	Light gray
Specific gravity	2.1
Specific surface area	$16.7 \ m^2/g$
PH	6.5
Chemical analysis	**Value**
$Si\ O_2$	94.30 - 92.0
$Fe_2\ O_3$	0.84 - 1.5
$Al_2\ O_3$	0.24 - 1.5
$Mg\ O$	0.50 - 1.0
$Ca\ O$	0.25 - 0.5
$H2\ O$	0.37 - 1.0

Table (5) Physical and Chemical Properties of Fly Ash.

Physical properties	Value
Colors	Light gray
Specific gravity	2.2
Specific surface area	$8\ m^2/g$
PH	1.2
Chemical analysis	
$Si\ o_2$	53.0
$Al_2\ o_3$	34.0
$Fe_2\ o_3$	3.5
$Mn_2\ o_3$	0.2
$Ca\ o$	4.5
$Mg\ o$	1.5
$K_2\ o$	0.6
So_3	0.3

Table (6) Properties of Viscosity Enhancing Agent Viscocrete (5 - 400).

Properties	Value
Density	1.11
PH – value	8.0
Appearance	Turbid liquid
Chloride content	Zero

Table (7) Typical Physical, Chemical and Mechanical Properties of Polyester Resin (2504 APT-5).

Property	Value
Appearance	Light yellowish turbidity
Styrene monomer content, %	37-39
Viscosity-Brookfield at 25°C #3 spindle at 60pm, cps	350-450
Thixotropic index at 25°C Brookfield LVT, #3 spindle 6/60rpm	1.0-2.0
Typical gel data	
Room temperature cure at 25 °C, 1% MEKPO (55%) 0.5% Cobalt octoate (CO. 6%)	
Gel time, mins.	18
Gel to peak exotherm, mins.	12
Total time to peak exotherm, mins.	30
Peak exotherm temperature, °C	150
Clear casting, ETERSET2504APT-S	
Barcol hardness	44
Tensile strength, Kg/cm^2	600
Flexural strength, Kg/cm^2	1100
Flexural modulus, Kg/cm^2	3.0×10^4
Heat distortion temperature, °C	70

Table (8) Mechanical Properties of Carbon Fiber, Glass Fiber and Steel Plates.

Strengthening System	Mechanical Property	Value
Carbon fiber	Ultimate tensile strength f_{fu}	960 N/mm^2
	Rupture strain ε_{fu}	1.33%
	Modulus of elasticity of FRP laminates E_f	73.100 N/mm^2
Glass fiber	Ultimate tensile strength f_{fu}	600 N/mm^2
	Rupture strain ε_{fu}	2.24%
	Modulus of elasticity of FRP laminates E_f	26.130 N/mm^2
Steel plate	Ultimate tensile strength f_{fu}	225 N/mm^2
	Rupture strain ε_{fu}	1. 4%
	Modulus of elasticity of FRP laminates E_f	210.000 N/mm^2

Table (9) Mix Constituents by weight in kg of SCC .

Cement	Sand	Dolomite	Water	Fly ash	Silica fume	VEA
400	1000	1000	133	40	40	10

Table (10) Experimental Program Designed for Strengthening of Self-Compacted Reinforced Concrete Beams by Using Different FRP and Steel Systems.

Beam code	Strengthening System	No. of Layer	Geometry
Bc	Control beam	-	
B1	Carbon fiber	1 Layer carbon fiber	
B2	Glass fiber + Carbon fiber	1 Layer Glass Fiber + 1 Layer Carbon Fiber	
B3	Glass fiber	3 Layers Glass Fiber	
B4	Carbon fiber + Glass fiber	2 layers Glass Fiber + 1 Layer Carbon Fiber	
B5	Polypropylene	4 Layers	
B6	Glass fiber	6 Layers Glass Fiber	
B7	Steel plate thickness 1mm and 50 mm width	1 Layer	
B8	Steel plate thickness 2mm and 50 mm width	1 Layer	

Khaled M. Heiza

Table (11)The Results of the Cubic Compressive Strength F_{cu} of the Tested SCC Specimens After 28 Days

No. of sample	Failure load (KN)	Failure stress P/A (Kg/cm²)	Average value (Kg / cm²)
1	350	350	
2	310	310	
3	330	330	333
4	360	360	
5	310	310	
6	340	340	
1	370	370	
2	380	380	
3	340	340	348
4	310	310	
5	360	360	
6	330	330	
1	400	400	
2	350	350	
3	340	340	359
4	385	385	
5	320	320	
6	359	359	
1	320	320	
2	370	370	
3	300	300	342
4	280	280	
5	440	440	
6	342	342	

Table (12) The Results of the Splitting Tensile Strength F_t of the Tested SCC Specimens After 28 days.

No. of sample	Failure load (KN)	Failure stress P/A (Kg/cm²)	Average value (Kg / cm²)
1	150	48.7	
2	170	55.2	
3	130	42.2	47.05
4	120	38.9	
5	170	55.2	
6	130	42.2	
1	100	32.5	
2	120	38.9	
3	170	55.2	42.6
4	135	43.8	
5	132	42.6	
6	132	42.6	
1	100	32.5	
2	100	32.5	
3	120	38.9	40.3
4	150	48.7	
5	155	50.3	
6	120	38.9	

Table(13) The Results of Flexural Strength F_b of the Tested SCC Specimens after 28 days.

Load (kg)	M max (kg. cm)	F_b (Kg / cm^2)	average value (kg /cm^2)
1050	13125	78.75	
1050	13125	78.75	82
1180	14750	88.5	
1050	13125	78.75	
1170	14625	87.75	78.75
930	11625	69.75	
1300	16250	97.5	
1100	13750	82.5	86.25
1050	13125	78.75	

Table (14) Test Results Of (P-crack, P-Ultimate, Deflection and Rotation) of Strengthened Self-Compacted Reinforced Concrete Beams.

Beam code	P crack (ton)	P ultimate (ton)	Deflection (Δ) (mm)	Rotation (θ) (degree)
Bc	2.00	5.66	11.23	0.935
B_1	2.20	6.45	11.05	0.634
B_2	2.30	7.07	13.54	0.725
B_3	2.20	6.60	14.50	0.698
B_4	2.39	6.81	11.98	0.697
B_5	2.10	6.14	14.84	1.150
B_6	2.50	7.75	10.90	0.869
B_7	3.30	8.24	10.69	0.840
B_8	4.00	7.73	6.88	0.408

Table (15) Tests Results of (P-crack, P-Ultimate, Deflection and Rotation) of Strengthened Reinforced Concrete Beams Compared to the Control Beam (BC).

Beam code	P-crack (ton)	P-ultimate (ton)	Deflection (Δ) (mm)	Rotation (θ) (degree)
Bc	2.0	5.66	11.23	0.935
B1 (% Bc)	10% (Bc)	14% (Bc)	-2% (Bc)	-32% (Bc)
B2 (% Bc)	15% (Bc)	25% (Bc)	20% (Bc)	-28% (Bc)
B3 (% Bc)	10% (Bc)	16.6% (Bc)	29% (Bc)	-25% (Bc)
B4 (% Bc)	19.5% (Bc)	20.3% (Bc)	7% (Bc)	-25% (Bc)
B5 (% Bc)	5% (Bc)	8.5% (Bc)	32% (Bc)	22% (Bc)
B6 (% Bc)	25% (Bc)	36.9% (Bc)	-3% (Bc)	-7% (Bc)
B7 (% Bc)	65% (Bc)	45.6% (Bc)	-5% (Bc)	-10% (Bc)
B8 (% Bc)	100% (Bc)	36.6% (Bc)	-39% (Bc)	-55% (Bc)

Table (16) Test Results of Both Displacement Ductility Index and Curvature Ductility Index for the Self-Compacted Strengthened Reinforced Concrete Beams.

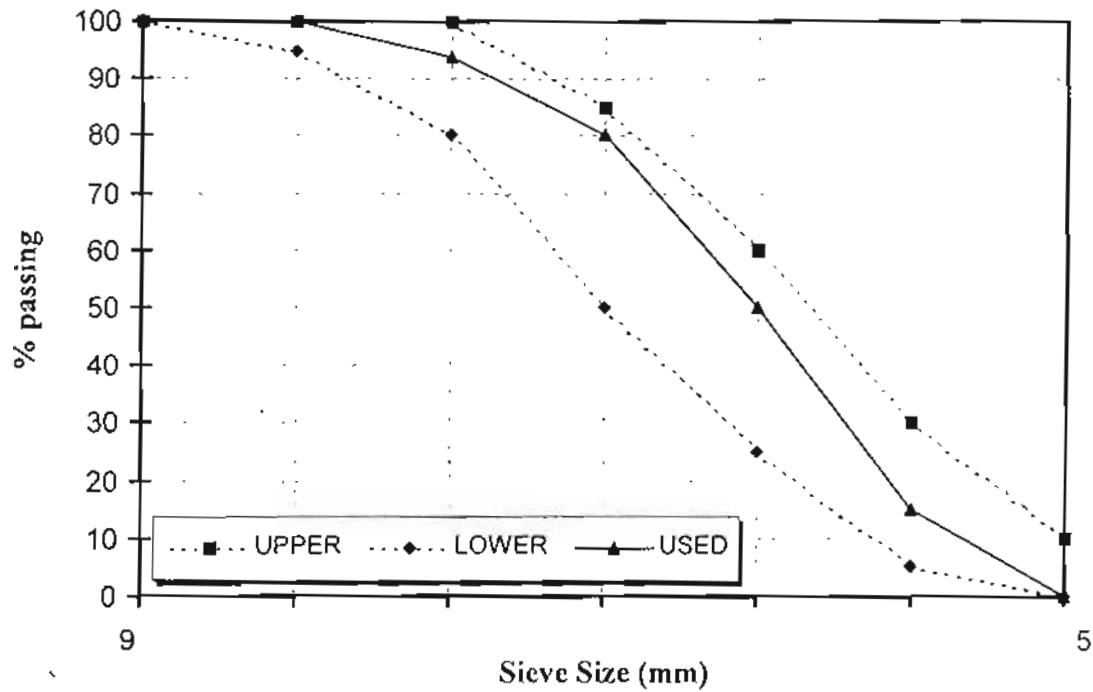| Beam code	Deflection (ΔY) (mm)	Rotation (θY) (degree)	Deflection (ΔU) (mm)	Rotation (θU) (degree)	Displacement ductility index (μd)	Curvature ductility index $(\mu \theta)$
Bc	2	0.25	11.23	0.935	5.6	3.74
B_1	1.9	0.23	11.05	0.634	5.8	2.75
B_2	1.6	0.15	13.54	0.725	8.5	4.8
B_3	1.6	0.23	14.50	0.698	9	3.03
B_4	1.5	0.22	11.98	0.697	8	3.16
B_5	1.4	0.16	14.84	1.150	10.6	7.2
B_6	1.6	0.12	10.90	0.869	4.36	7.2
B_7	1.6	0.18	10.69	0.840	3.2	4.7
B_8	1.0	0.15	6.88	0.408	6.88	2.72

Fig. (1) Grading of sand of F.M. 2.6
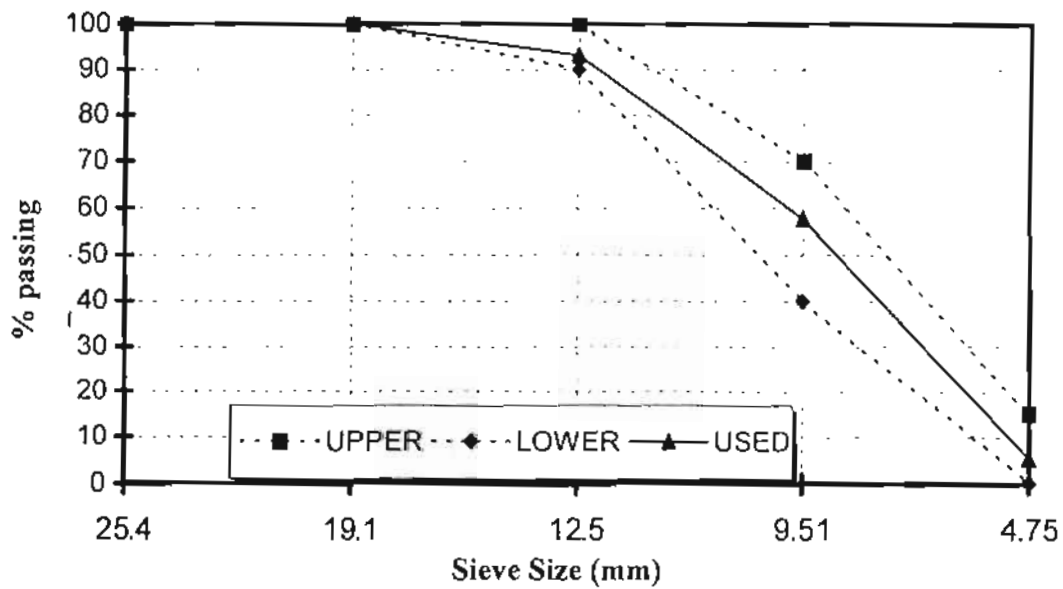
Fig. (2) Grading of dolomite of N.M.S 14 mm

```
┌─────────────────────────────────────┐
│         Clean the Beam Bottom        │
└─────────────────────────────────────┘
                    │
                    ▼
      ┌───────────────────────┐
      │     Mix the Resin      │
      └───────────────────────┘
                    │
                    ▼
┌─────────────────────────────────────────────────┐
│ Apply the Mixture to the GFRP and CFRP Wrapping  │
└─────────────────────────────────────────────────┘
                    │
                    ▼
┌───────────────────────────────────────────────────────────────┐
│ Bond the GFRP and CFRP Wrapping to Concrete and Compressed with │
│                    a Hard Rubbed Roller                         │
└───────────────────────────────────────────────────────────────┘
                    │
                    ▼
      ┌───────────────────────────────┐
      │   Remove the Excess of Mixture │
      └───────────────────────────────┘
                    │
                    ▼
      ┌───────────────────────────────┐
      │  Clean the GFRP and CFRP Wrapping │
      └───────────────────────────────┘
                    │
                    ▼
      ┌───────────────────────────────┐
      │       Curing of Mixture        │
      └───────────────────────────────┘
                    │
                    ▼
      ┌───────────────────────────────┐
      │        Check for Voids         │
      └───────────────────────────────┘
```
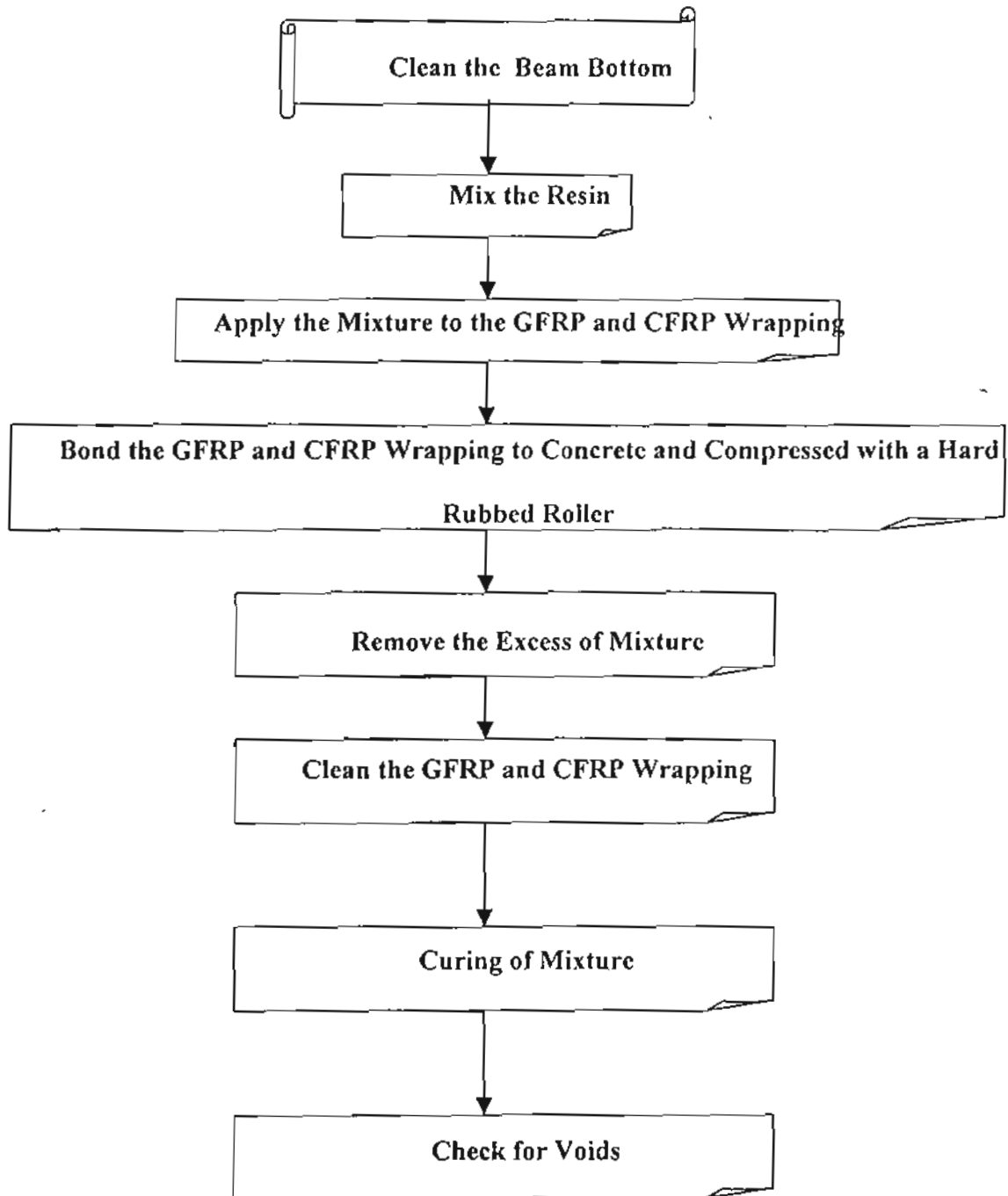
Fig.(3) Strengthening Process Sequences Used for Self-Compacted Reinforced Concrete Beams Strengthened by Using Hybrid System of (2 Layer GFRP+ 1 Layer CFRP).
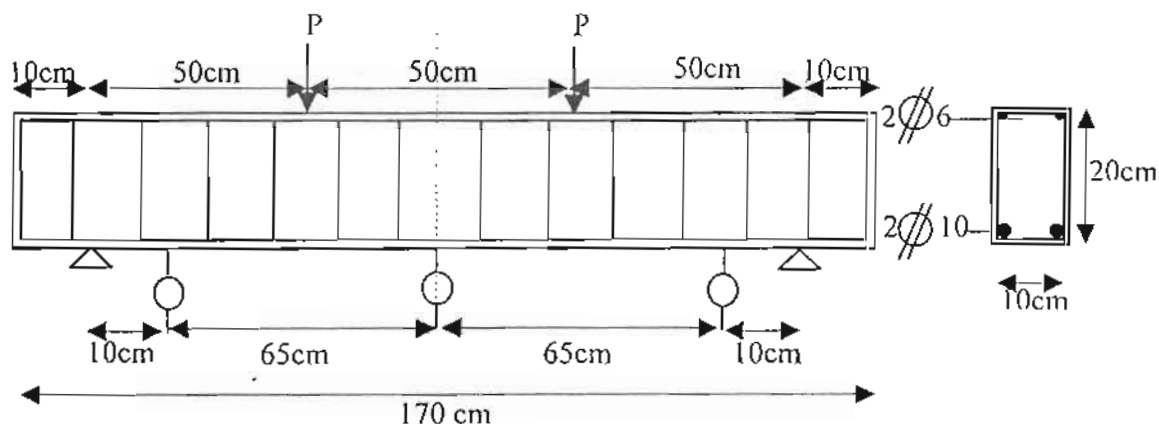
P   P

10cm   50cm   50cm   50cm   10cm

2Ø6

20cm

2Ø10

10cm

10cm   65cm   65cm   10cm

170 cm

Figure (4) Reinforcement Details of Reinforced Concrete Specimens.

Heading of testing machine

Dial gauges

Two Point Loading

Steel strip

Beam

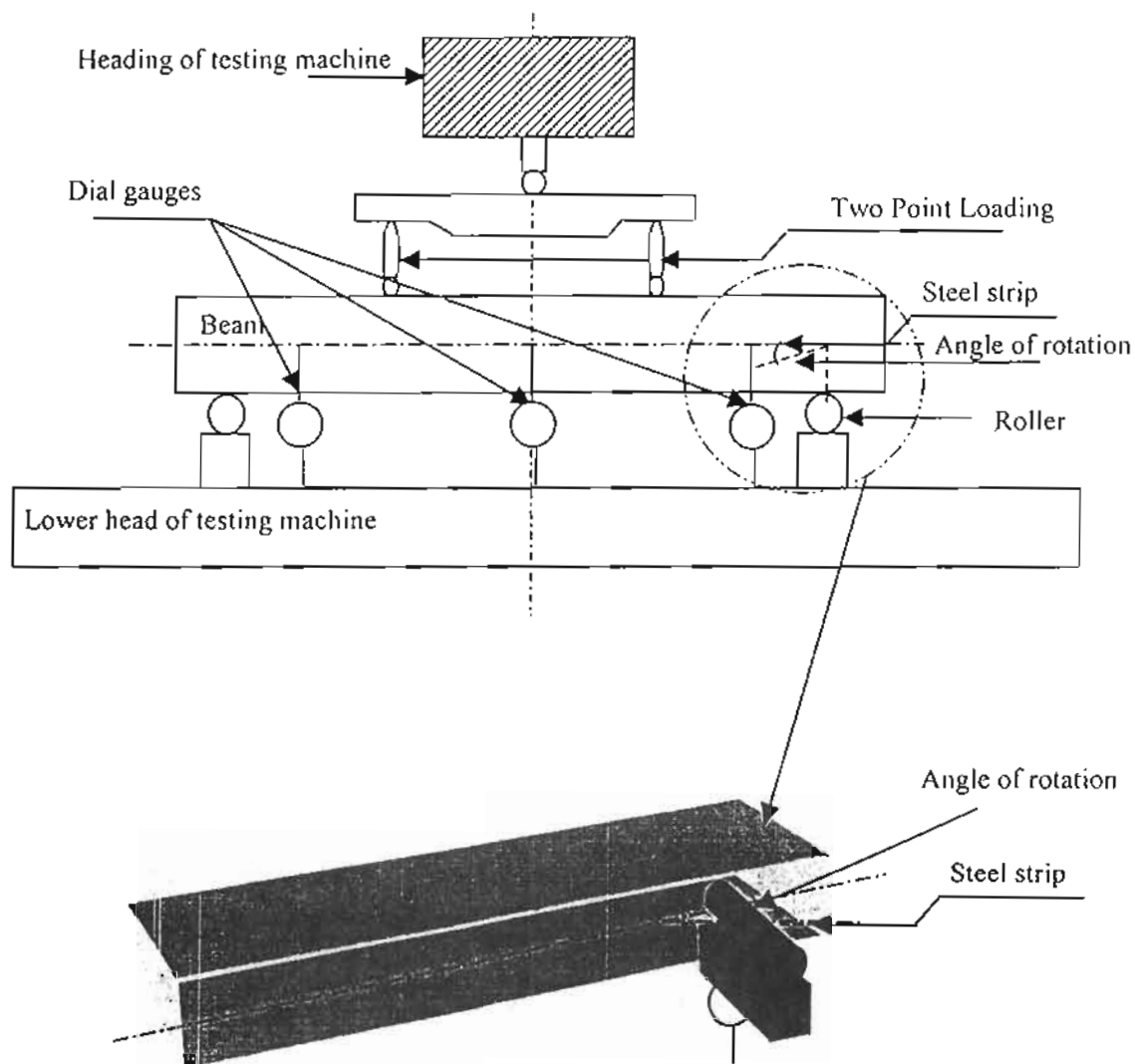Angle of rotation

Roller

Lower head of testing machine

Angle of rotation

Steel strip

Figure (5) Testing Machine and Test Set-Up.
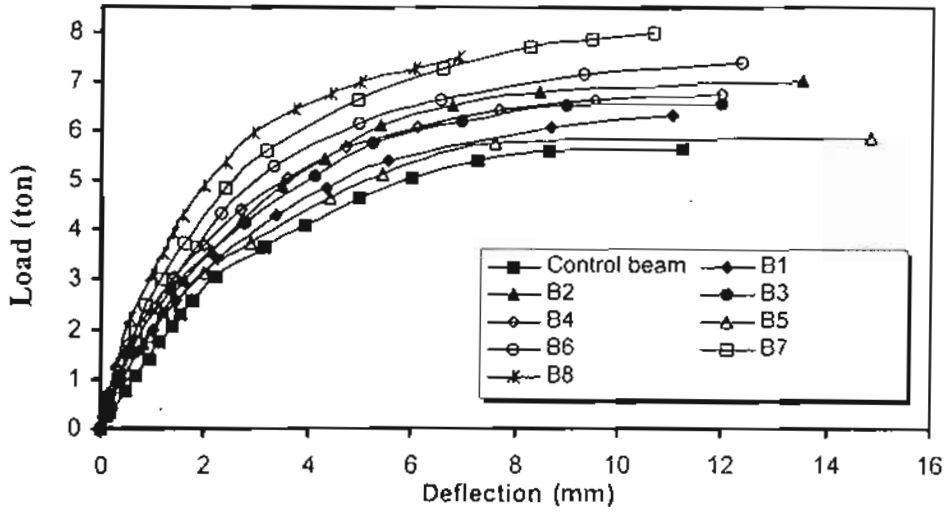
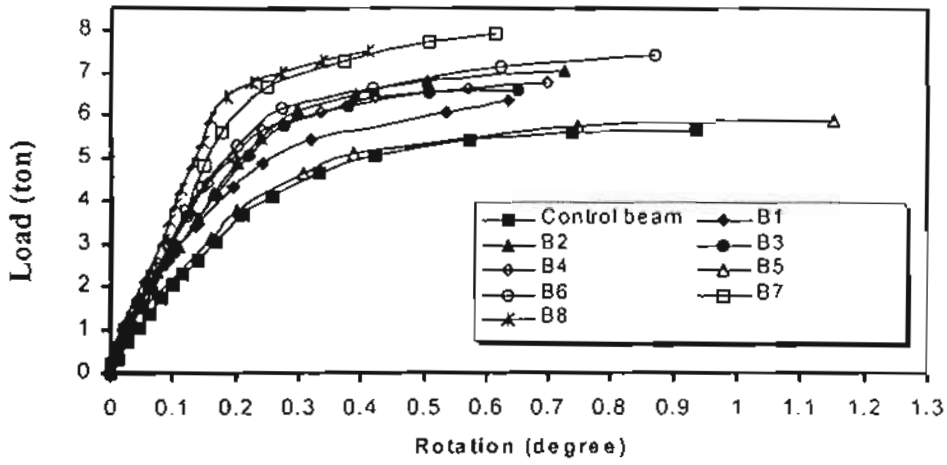Fig.(6) The load-deflection relationship for control beam
and beams strengthed with FRP and steel systems

Fig.(7) The load-rotation relationship for control beam and
beams strengthed by FRP and steel systems
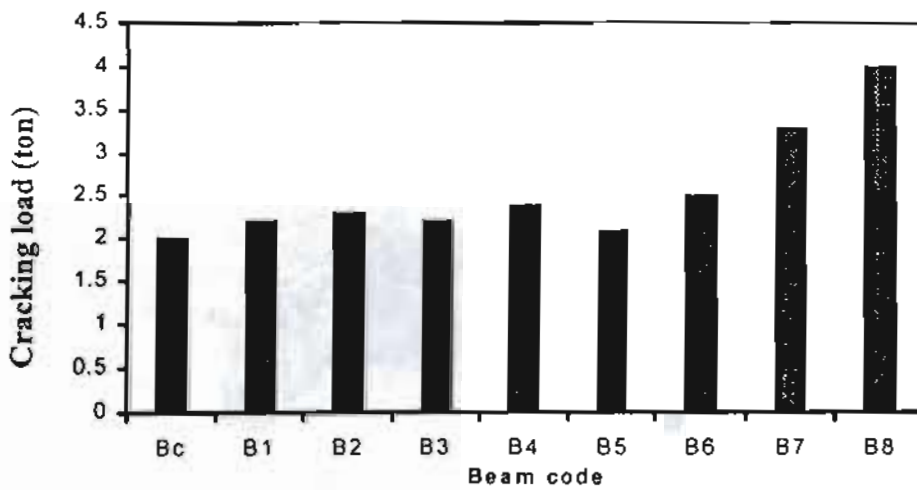
Fig.(8) initial cracking load for the tested Reinforced
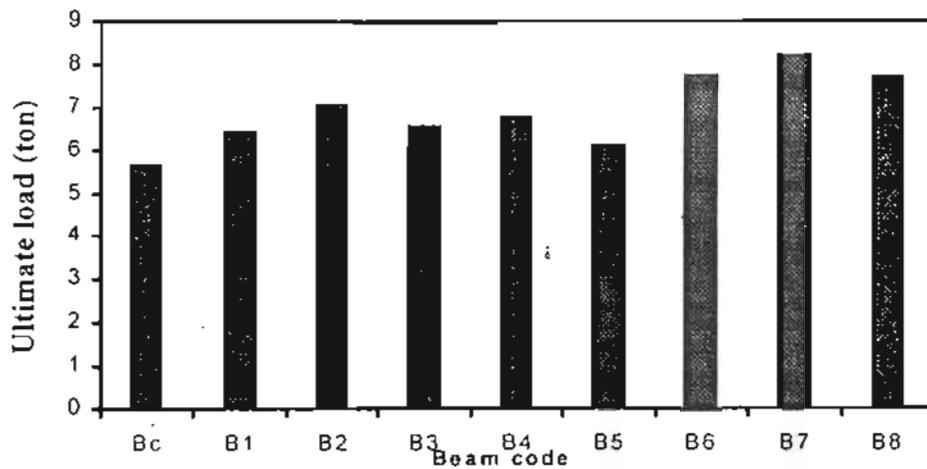concrete beams with different FRP and steel systems

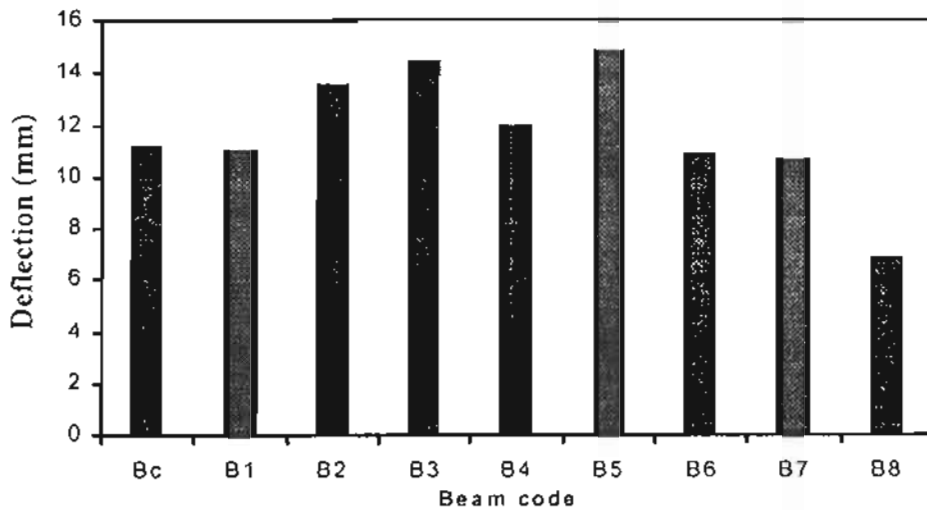Fig.(9) Ultimate load for the tested Reinforced concrete beams with different FRP and steel systems.

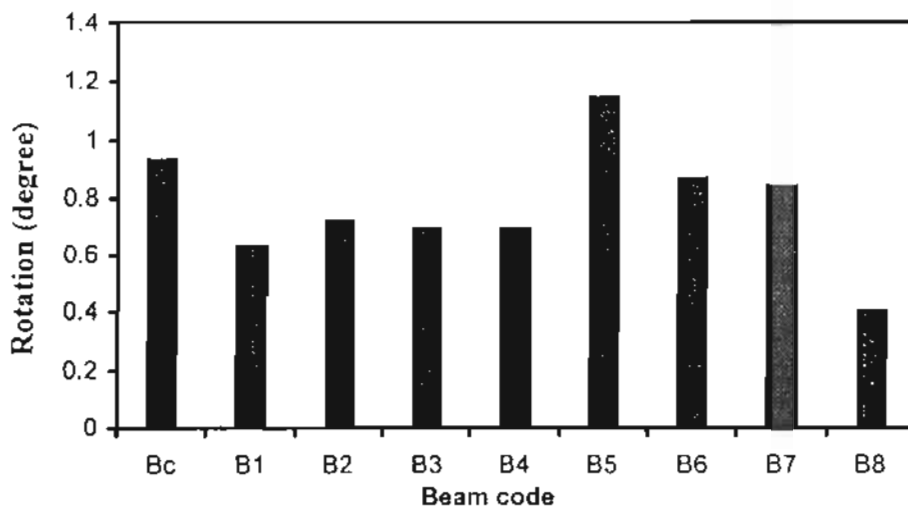Fig.(10) Deflection for the tested Reinforced concrete beams with different FRP and steel systems.

Fig. (11) Angle of roltation for the tested Reinforced concrete beams with different FRP and steel systems .
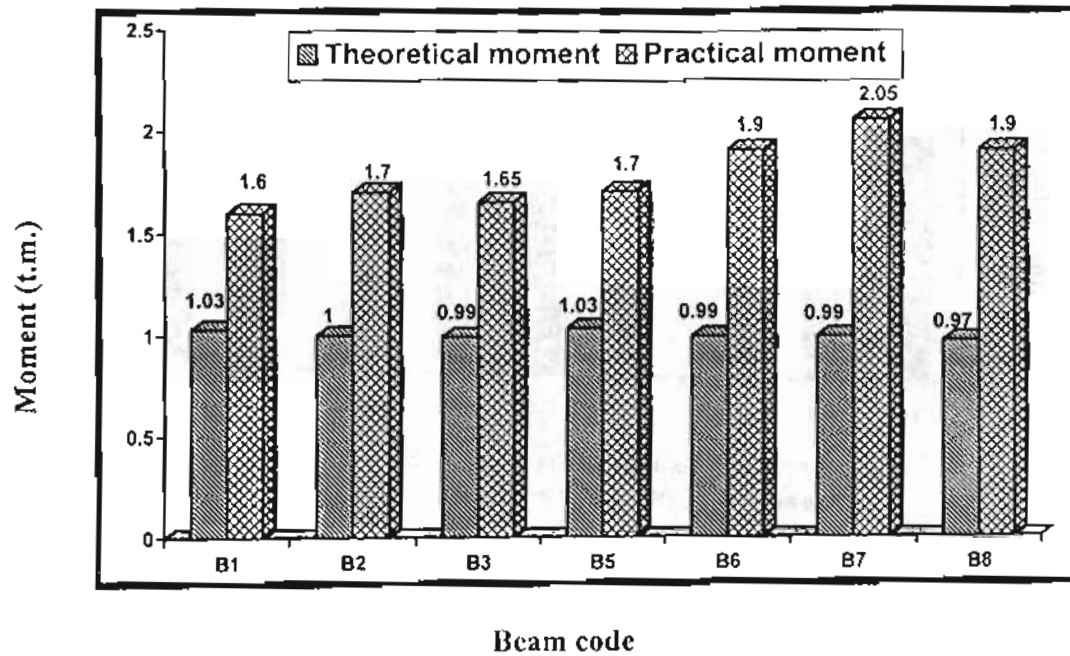
Khaled M. Heiza

Beam code
Fig. (12) Relationship Between Theoretical and Practical
Moments According to ACI 440. 2R-02